

Fabrication of submicrometric magnetic structures by electron-beam lithography

J. I. Martín,^{a)} Y. Jaccard, A. Hoffmann,^{b)} J. Nogués,^{c)} J. M. George,^{d)} J. L. Vicent,^{a)} and Ivan K. Schuller

Department of Physics, University of California–San Diego, La Jolla, California 92093-0319

(Received 14 January 1998; accepted for publication 31 March 1998)

Submicrometric magnetic structures have been fabricated by electron-beam lithography on Si substrates. High-quality patterns have been obtained with typical length scale of the structures in the range of 100 nm. The designed geometrical configurations are suitable for investigation of their physical properties by transport measurements in a controlled way. In particular, long chains of connected magnetic dots are useful to analyze magnetization reversal processes, whereas ordered arrays of isolated dots can be used to study pinning effects in superconducting films. © 1998 American Institute of Physics. [S0021-8979(98)05813-7]

I. INTRODUCTION

The fabrication of submicrometric magnetic structures with controlled geometries is very interesting both from the fundamental and applied physics points of view. Due to their well-defined geometry, these structures allow us to study different properties of the materials in a simple way. Moreover, as their small dimensions become comparable to the characteristic length scales of the material (e.g., magnetic domain walls), these structures can exhibit novel properties. Furthermore, submicrometric magnetic structures can play an important role in the design of new technological systems, as those related to magnetic recording media,^{1–3} due to the miniaturization trend in this field.

The recent development of new lithographic techniques has been crucial for the advancement of research in these submicrometric structures. Some of these techniques are (i) x-ray lithography,^{4,5} where the patterns are made using synchrotron radiation; (ii) scanning tunneling microscopy-assisted techniques,⁶ in which the tunneling current between the tip and the substrate is used to induce the deposition of metallic species in small and controlled areas; and (iii) electron-beam lithography, which is the most widely used,^{7–9} where the desired pattern is defined by an electron beam of a scanning electron microscope (SEM).

In this paper, we present the fabrication details of novel and different submicrometric structures of magnetic materials produced by electron-beam lithography and a subsequent lift-off process. The specific geometries have been designed to make the structures appropriate for physical properties studies using transport measurements. In particular, these small, controlled structures help in obtaining a further understanding of such diverse phenomena as magnetization reversal processes of magnetic particles or vortex pinning in superconductors.

II. ELECTRON-BEAM LITHOGRAPHY

The electron-beam lithography process used to produce the submicrometric structures consists of several sequential steps, as is schematically shown in Fig. 1. First, the desired pattern is drawn with the electron beam of a SEM onto a substrate [in our case, Si(100) or Si(111)] covered with an electron sensitive resist layer [Fig. 1(a)]. In particular, the resist we have used is a solution of 4% polymethylmethacrylate (PMMA) in trichlorobenzene, and it covers the substrate with a thickness of 300 nm. The microscope is a JEOL 6400 SEM in which a nanometer pattern generation system of nability has been installed, so that the electron beam is controlled from an external computer to write in the PMMA the previously programmed pattern. Working with an acceleration voltage of 30–36 kV, the electron-beam current has been varied from 30 pA to 1 nA depending on the type of pattern. In general, each pattern is defined over a $50\ \mu\text{m} \times 50\ \mu\text{m}$ region; within this size the deflection of the beam is small and the focus remains good.

After writing the pattern, the Si substrate with PMMA is developed at 16 °C for 30–35 s in a 3:1 mixture of developer and ethanol. In this way, those PMMA regions which were exposed to the electron beam are removed from the substrate [Fig. 1(b)]. Afterwards, the desired magnetic material is grown at room temperature on top of this PMMA template [Fig. 1(c)]. In particular, we have used as a magnetic material the ferromagnetic transition metals: iron, cobalt, and nickel. They have been deposited either by sputtering (Fe and Ni) or by electron-beam evaporation (all of them) up to a total thickness of 40–50 nm, which has been calibrated by low-angle x-ray diffraction.

Finally, a lift-off process is carried out. The sample is immersed in acetone, in order to dissolve the PMMA template remaining on the substrate. This procedure removes also the magnetic material deposited on top of the PMMA layer. Hence, the magnetic layer remains only where it has been grown directly on the substrate (i.e., in those regions which have been previously defined by the electron beam), so that the desired pattern is obtained [Fig. 1(d)].

^{a)}On leave from Universidad Complutense, 28040 Madrid, Spain.

^{b)}Electronic mail: hoffmann@ucsd.edu

^{c)}Present address: Universitat Autònoma de Barcelona, 08193 Bellaterra, Spain.

^{d)}Present address: CNRS–Thomson CSF, 91404 Orsay, France.

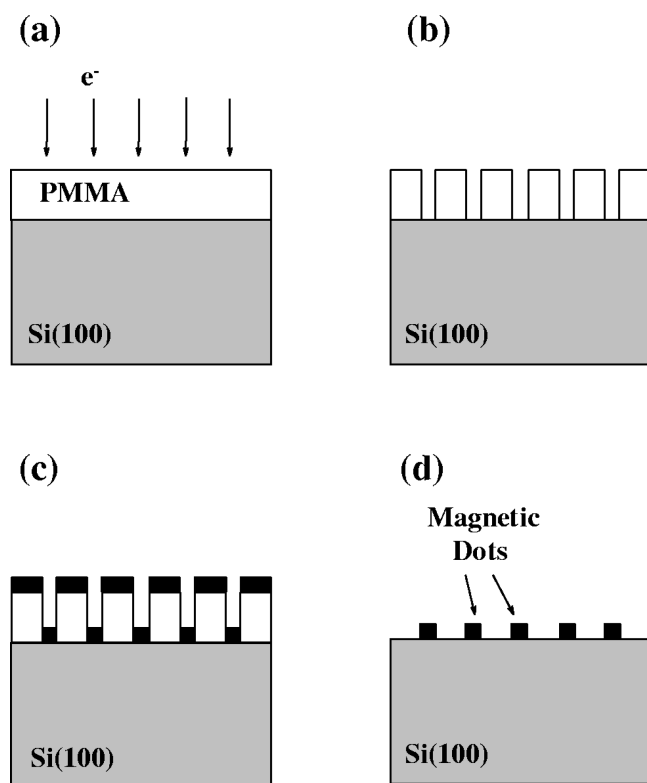


FIG. 1. Sketch of the electron-beam lithography process. (a) Writing the designed pattern using the SEM. (b) Development of the PMMA. (c) Growth of the magnetic layer. (d) Lift-off.

High-quality reproducible patterned samples result at the end of this electron-beam lithography process. Some examples of the fabricated structures appear in Fig. 2, where SEM pictures are presented. In Fig. 2(a) an array of Ni lines is shown; the lines are straight, parallel, separated by 500 nm, and have a width of ≈ 100 nm. Figure 2(b) presents a micrograph of circular isolated dots of cobalt, which are very regular in size and shape, with a diameter smaller than 100 nm.

Using these conditions, we have designed two different kinds of submicrometric structures for hysteresis studies of magnetic materials and pinning investigations in superconductors. These patterns are long connected chains of magnetic dots and ordered arrays of separated dots, which are described in more detail in the following sections.

III. CHAINS OF MAGNETIC DOTS

The first type of structures that we have fabricated and studied consists of long and continuous chains of magnetic dots connected by narrow constrictions, so that an electrical current can be applied along them. This allows investigation of their magnetic behavior using transport measurements. This technique overcomes difficulties associated with the small total volume of these submicrometric samples, which makes the total magnetic moment of a typical pattern too small to be detected by standard magnetometry techniques. Besides, chains of dots have been widely used in theoretical models to simulate magnetization reversal processes.¹⁰

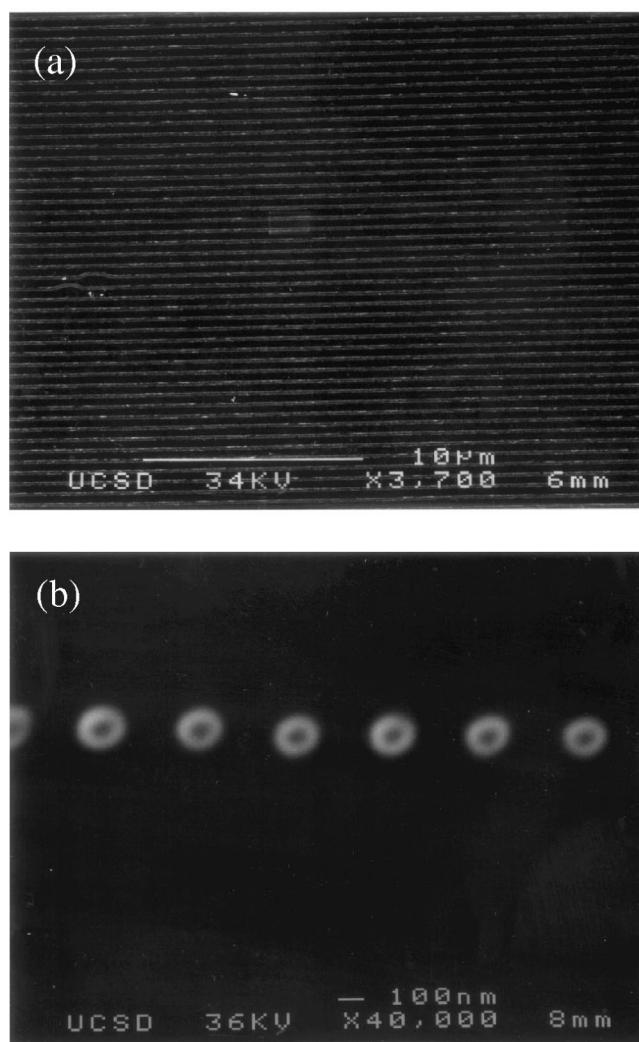


FIG. 2. SEM pictures of several submicrometric structures prepared by electron-beam lithography. (a) Parallel lines of nickel separated by 500 nm. (b) Isolated Co dots with diameters around 100 nm.

Therefore, our patterns are ideally suited for the study of such processes in an easy and controlled fashion and provide an experimental realization of these models.

Figure 3(a) is a SEM image of a typical sample, showing well-defined chains of Ni dots. The dot diameter is approximately 400 nm, which is the same as the distance between the dot centers, and the thickness is 45 nm. In general, each chain is made of 50 dots up to a total length of 20 μm . During the fabrication process, the electron-beam current of the microscope has been varied between 60 and 300 pA, adjusting it carefully in order to obtain narrow connections between the dots of around 100 nm in width. The length scale of these structures is comparable to typical domain-wall sizes of ferromagnetic transition metals,¹¹ so that interesting properties can be expected as each dot should only contain a few magnetic domains or even be a monodomain.

The chains of dots have been arranged in different geometrical configurations. First, straight chains have been prepared in sets ranging from 1 to 25 parallel chains separated by 2 μm from each other. Then, more complicated structures, such as the one shown in Fig. 3(b), have been designed

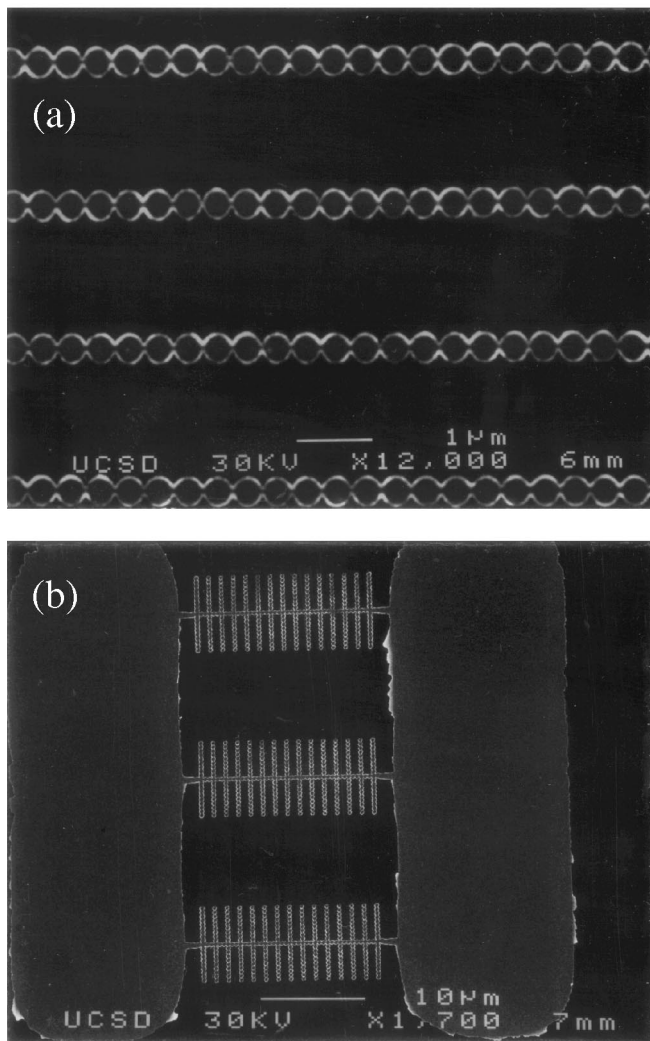


FIG. 3. (a) SEM micrograph of long chains of connected Ni dots with diameters of 400 nm. (b) SEM picture of chains of Ni dots with perpendicular branches; the rectangular regions for the contacts of the transport measurements are also visible.

in order to control and modify the influence of shape anisotropy in the magnetization reversal processes. In all these cases, rectangular pads of the same material have been defined at the end of the chains to make the contacts for the transport measurements, as can be seen in Fig. 3(b). For that purpose, conventional optical lithography is performed on top of the pattern, so that, after growing a silver layer, the contacts are obtained by a lift-off procedure.

These long chains of submicrometric magnetic dots present transport properties like those shown in Fig. 4 for a single chain of Fe dots. The temperature dependence of the resistance has a metallic behavior even for only one chain of dots in the sample (inset of Fig. 4), indicating the metallic character of the constrictions between the dots. The magnetic-field dependence of the resistance appears in Fig. 4 for the same sample of Fe dots, measured with the field applied parallel to the substrate plane but perpendicular to the chain (and, therefore, perpendicular to the current). At high enough fields $R(H)$ presents a parabolic behavior, which is typical of metallic films. In the low-field region, the

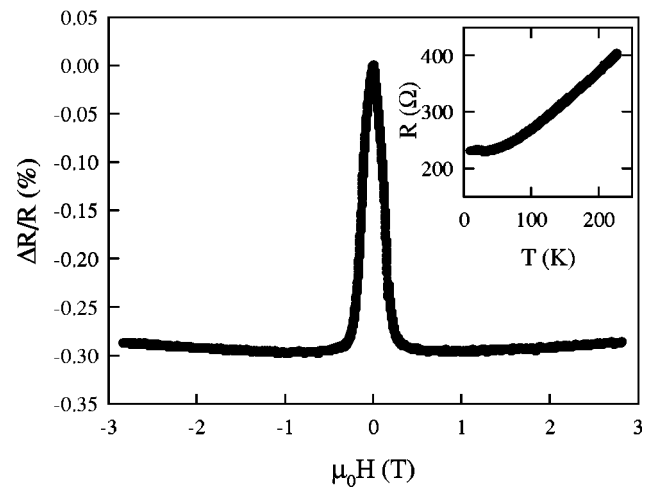


FIG. 4. Magnetoresistance as a function of field for one chain of 400 nm diam Fe dots at $T=10$ K; H is applied in the sample plane but perpendicular to the chain. The inset shows the $R(T)$ curve of the same pattern.

characteristic negative magnetoresistance of these ferromagnetic materials¹² is found. The analysis of the shape of these magnetoresistance hysteresis loops in comparison with those of unpatterned single films has been used to get further understanding of magnetization reversal processes.¹³

IV. ORDERED ARRAYS OF DOTS

There are many aspects that can be addressed in the study of ordered arrays of magnetic dots, such as magnetic coupling¹⁴ or the fabrication of magnetic recording media.³ Also, these submicrometric magnetic structures are interesting in the field of superconductivity. The characteristic lengths of superconducting materials, such as the penetration depth λ and the coherence length ξ , are in the submicron range. Therefore, the fabrication of controlled defects in superconductors with sizes comparable to the vortex core (i.e., comparable to ξ) is interesting, since they are promising candidates for strong pinning centers for the vortex lattice.¹⁵ For these studies, we have fabricated regular arrays of isolated magnetic dots in order to study their pinning effect on Nb thin films.

Figure 5 shows a SEM picture of an array of magnetic dots with a hexagonal structure. We have also prepared arrays with other geometrical configurations (square or rectangular) to analyze and compare anisotropic properties. In particular, the dots in Fig. 5 have been made with an electron-beam current of 50 pA and have a diameter of 200 nm, which are typical values for the arrays we have studied. The lattice spacing between dots has been varied between 0.3 and 1 μm .

To study the pinning effect of magnetic dot arrays on superconductors, a niobium film has been grown on top of the arrays of magnetic dots, either by sputtering or molecular beam epitaxy, with thickness varying from 50 to 100 nm. To carry out transport measurements, a 40 μm wide bridge is defined by optical lithography and reactive ion etching. The Nb film prepared under these conditions shows metallic be-

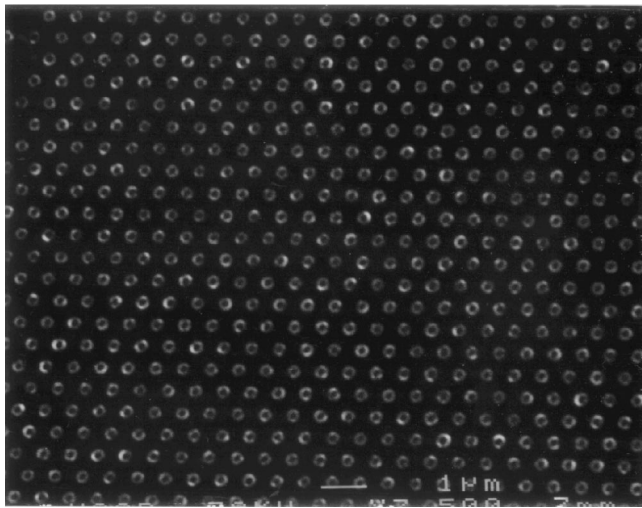


FIG. 5. SEM picture of a hexagonal array of Fe dots. The lattice parameter is 600 nm, and the dot diameter is 200 nm.

havior and a sharp superconducting transition as shown in Fig. 6(a). The critical temperature T_C is in the range 7.5–8.5 K, depending on the niobium thickness.

The influence of the array of magnetic dots is clearly observed in the mixed state. In Fig. 6(b) we have plotted the field dependence of the resistivity for two different samples at similar reduced temperature ($T/T_C \approx 0.98$); in one of them (solid symbols), the Nb film is on top of a hexagonal array of Fe dots with a lattice spacing of $d = 600 \pm 10$ nm. On the other (open symbols), the hexagonal array is made of Ni dots with $d = 410 \pm 10$ nm. In both cases sharp minima in the resistivity appear at regular field intervals. The distance between two consecutive minima ΔB is constant for each sample and is clearly smaller for the film grown on the array with larger d [$\Delta B = 6.2 \pm 0.6$ mT for the Fe array ($d = 600$ nm) and $\Delta B = 14.1 \pm 0.4$ mT for the Ni one ($d = 410$ nm)]. The number of observed minima is different in each sample, probably due to the difference in H_{C2} . The minima can be attributed to a matching effect between the vortex lattice and the ordered array of magnetic dots that induces a synchronized pinning effect and, therefore, a reduction in the dissipation.¹⁶ The spacing of the vortex lattice a_0 depends on the magnetic field according to the well-known Abrikosov formula¹⁷ $a_0 = \sqrt{1.075\Phi_0/B}$, where Φ_0 is the flux quantum. Therefore, the matching condition $a_0 = d$ is fulfilled for $B = 6.7 \pm 0.2$ mT in the first sample and $B = 14.2 \pm 0.7$ mT in the second. These values are in good agreement with the experimentally observed magnetic field of the first minima. Higher-order peaks correspond to an integer number of vortices per unit cell of the dot array.

V. CONCLUSIONS

In summary, different new submicrometric structures of magnetic materials have been produced by electron-beam lithography followed by a lift-off process. The obtained patterns present sharp and reproducible shapes and sizes as small as 100 nm. The designed structures allow controlled studies of different magnetic and superconducting properties

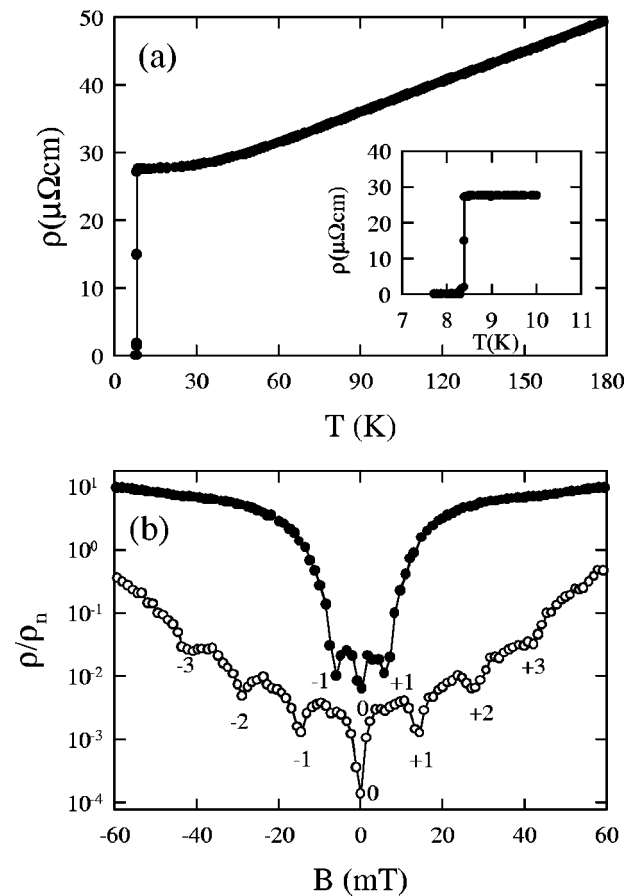


FIG. 6. (a) Resistivity vs temperature of a 100 nm Nb film grown on top of a hexagonal array of Ni dots. Inset shows the transition in an expanded scale. (b) Field dependence of resistivity at $T/T_C \approx 0.98$ in 100 nm Nb films grown on two different patterns: solid symbols, hexagonal array of Fe dots with $d = 600$ nm; and open symbols, hexagonal array of Ni dots with $d = 410$ nm. The data have been normalized by the normal state resistivity ρ_n and the top curve has been vertically displaced by a factor of 10 for clarity. The order of the minima in the resistivity are indicated in the figure.

of materials using transport measurements. In particular, we have fabricated long chains of magnetic dots, suitable to study the magnetization reversal processes. Furthermore, ordered arrays of magnetic dots have been prepared to investigate their influence on superconducting Nb films, for which an enhanced pinning effect of the vortex lattice by the array of dots has been found.

ACKNOWLEDGMENTS

This work has been supported by the U.S. Department of Energy and Air Force Office of Scientific Research. Two of the authors (J.I.M. and J.N.) acknowledge a postdoctoral fellowship from the Spanish MEC. One of the authors (Y.J.) acknowledges a postdoctoral fellowship from the Swiss NSF. The authors appreciate useful discussions with A. Herzog, F. Sharifi, A. Katz, P. Xiong, S. Appelbaum, and M. Vélez.

¹S. Manalis, K. Babcock, J. Massie, V. Elings, and M. Dugas, *Appl. Phys. Lett.* **66**, 2585 (1995).

²J. L. Simonds, *Phys. Today*, **48**, April 26 (1996).

- ³S. Y. Chou, P. R. Krauss, and L. Kong, *J. Appl. Phys.* **79**, 6101 (1996).
- ⁴F. Rousseaux, D. Decanini, F. Carcenac, E. Cambil, M. F. Ravet, C. Chappert, N. Bardou, B. Bartenlian, and P. Veillet, *J. Vac. Sci. Technol. B* **13**, 2787 (1995).
- ⁵M. Hehn, K. Ounadjela, J.-P. Bucher, F. Rousseaux, D. Decanini, B. Bartenlian, and C. Chappert, *Science* **272**, 1782 (1996).
- ⁶D. D. Awschalom, M. A. McCord, and G. Grinstein, *Phys. Rev. Lett.* **65**, 783 (1990).
- ⁷J. F. Smyth, S. Schultz, D. R. Fredkin, D. P. Kern, S. A. Rishton, H. Schmid, M. Cali, and T. R. Koehler, *J. Appl. Phys.* **69**, 5262 (1991).
- ⁸A. Maeda, M. Kume, T. Ogura, K. Kuroki, T. Yamada, M. Nishikawa, and Y. Harada, *J. Appl. Phys.* **76**, 6667 (1994).
- ⁹K. J. Kirk, J. N. Chapman, and C. D. W. Wilkinson, *Appl. Phys. Lett.* **71**, 539 (1997).
- ¹⁰I. S. Jacobs and C. P. Bean, *Phys. Rev.* **100**, 1060 (1955).
- ¹¹B. D. Cullity, *Introduction to Magnetic Materials* (Addison-Wesley, Reading, MA, 1972).
- ¹²T. R. McGuire and R. I. Potter, *IEEE Trans. Magn.* **11**, 1018 (1975), and references therein.
- ¹³J. I. Martín, J. Nogués, I. K. Schuller, M. J. Van Bael, K. Temst, C. Van Haesendonck, V. V. Moshchalkov, and Y. Bruynseraede, *Appl. Phys. Lett.* **72**, 255 (1998).
- ¹⁴C. Mathieu *et al.*, *Appl. Phys. Lett.* **70**, 2912 (1997).
- ¹⁵A. M. Campbell and J. E. Evetts, *Adv. Phys.* **21**, 199 (1972).
- ¹⁶J. I. Martín, M. Vélez, J. Nogués, and I. K. Schuller, *Phys. Rev. Lett.* **79**, 1929 (1997).
- ¹⁷M. Tinkham, in *Introduction to Superconductivity* (McGraw-Hill, New York, 1975), p. 134.